# Wideband Characteristic Basis Functions in Radiation Problems

*Andrzej A. KUCHARSKI*

Inst. of Telecommunications, Teleinformatics and Acoustics, Wroclaw University of Technology,
Wybrzeze Wyspianskiego 27, 50-370 Wroclaw, Poland

andrzej.kucharski@pwr.wroc.pl

**Abstract.** *In this paper, the use of characteristic basis function (CBF) method, augmented by the application of asymptotic waveform evaluation (AWE) technique is analyzed in the context of the application to radiation problems. Both conventional and wideband CBFs are applied to the analysis of wire and planar antennas.*

## Keywords

Asymptotic waveform evaluation, characteristic basis functions, integral equations, moment methods.

## 1. Introduction

The characteristic basis function method [1], [2] is a powerful tool enabling efficient solution of large electromagnetic problems without the need of solving large matrix equations. In the original scheme, the computations are performed at a single frequency. An extension to the CBF method has been proposed, leading towards fast frequency sweep analysis [3] – [5]. In this approach, basis functions constructed at several frequency points are used as a universal set to be used in a given frequency band. Another attitude is that proposed in [6], where original CBF method has been combined with asymptotic waveform evaluation [7] – [9].

Here, we apply the attitude similar to [6], i.e. we construct the wideband approximation to primary, secondary and tertiary characteristic basis functions, using AWE method. However, the results presented in [6] concern two dimensional scattering problems, where the domains associated with CBFs are confined to single objects (cylinders) in multiple-object scattering. Here, we consider three-dimensional problems, concerning radiation phenomena, where one larger object (antenna) is sub-divided into several, overlapping regions. The results are compared in terms of current/input impedance data, in contrast to far-field calculation given in [6].

In the rest of this paper, we first outline the theory of wideband CBFs (AWE-CBFs [6]), then present computational examples, which prove the correctness of the procedure, and give some deeper insight into its details.

## 2. Construction of Wideband CBFs

### 2.1 Characteristic Basis Functions

Let's assume that we solve an electromagnetic radiation or scattering problem using integral-equation/method-of-moments (IE/MoM) approach. At the final stage, we arrive at the matrix equation of the form:

$$\boldsymbol{Z} \cdot \boldsymbol{I} = \boldsymbol{V} \tag{1}$$

where $\boldsymbol{Z}$ is the moment (impedance) matrix, $\boldsymbol{I}$ is the vector of unknown coefficients describing the approximation of the source distribution, and finally $\boldsymbol{V}$ is the vector dependent on the excitation.

In CBF method [1], [2], we divide the domain over which sources are approximated, into a set of (say) $M$ smaller subdomains. If a subdomain has a common boundary with other subdomains, we extend it with a properly chosen margin, into the area of those neighboring parts, forming so-called extended subdomain.

On each extended subdomain $i$, we compute a *primary* basis function $\boldsymbol{Jp}^{(i)}$, by solving a smaller problem, in which we treat the corresponding fragment of the analyzed structure as isolated from the rest, and only excited by the external incident field. This simply means that we use a proper sub-matrix of $\boldsymbol{Z}$, as well as a part of $\boldsymbol{V}$ vector:

$$\boldsymbol{Z}_e^{(i)} \cdot \boldsymbol{Jp}^{(i)} = \boldsymbol{V}^{(i)}. \tag{2}$$

For the localized excitation arising in radiation problems, it may happen that $\boldsymbol{V}^{(i)}$ vectors for some subdomains have only zero entries. In such cases, we may introduce special "artificial" excitations allowing to find primary CBFs [2], or simply – which is the case here – we may not associate primary basis functions with such subdomains.

When primary CBFs for each excited sub-region are found, we treat them as sources influencing other parts of the structure, and compute for each block $i$, a set of *secondary* CBFs $\boldsymbol{Js}_n^{(i)}$, solving equations of the type:

$$\boldsymbol{Z}_e^{(i)} \cdot \boldsymbol{Js}_n^{(i)} = -\boldsymbol{Z}^{(i,n)} \cdot \boldsymbol{Jp}^{(n)}, \quad (i \neq n). \tag{3}$$

Above, $\boldsymbol{Z}^{(i,n)}$ is the sub-matrix of $\boldsymbol{Z}$ relating sources in $n$-th subdomain to the fields at $i$-th subdomain, and $\boldsymbol{Jp}^{(n)}$ is (already computed from (2)) primary CBF for the block $n$.

The number of secondary CBFs for each block is equal to the number of primary CBFs if there is no primary CBF associated with this block, or to the number of primary CBFs minus 1, if there exists a primary CBF associated with the considered subdomain. If the excitation block overlaps with the block in which we compute secondary basis function, we don't take into account the overlapping parts of sources.

Finally, we compute tertiary basis functions $\boldsymbol{Jt}_{j,n}^{(j)}$ (called second secondary CBFs in [6]), using the formula:

$$\boldsymbol{Z}_e^{(i)} \cdot \boldsymbol{Jt}_{j,n}^{(i)} = -\boldsymbol{Z}^{(i,j)} \cdot \boldsymbol{Js}_n^{(j)}, \quad (i \neq j). \tag{4}$$

Next, we limit the CBFs to the original (not extended) subdomains. It is convenient to write those CBFs as vectors with the full size of $\boldsymbol{I}$ appearing in (1), just filling the rest of entries with zeros.

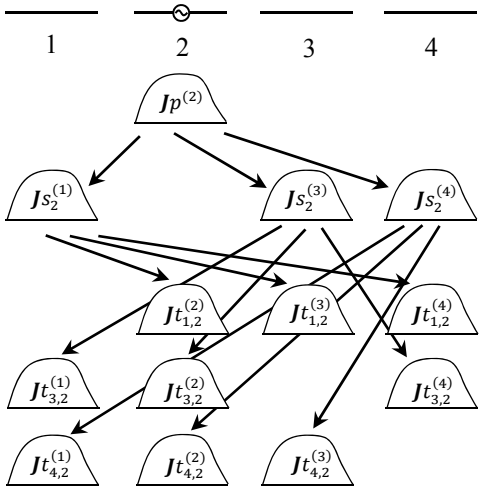


**Fig. 1.** Primary, secondary, and tertiary characteristic basis function for four sub-domains, one of which is excited.

In Fig. 1 we show the example interactions in the problem with $M = 4$ subdomains, from which one contains a localized excitation. For the sake of illustration the subdomains are shown as separate regions, although in general they can be parts of one lager structure. For the situation with one of $M$ subdomains excited the total number of CBFs is equal to $M^2 - M + 1$.

Please note, that secondary and tertiary CBFs defined here are not the same as introduced in [6], where for each sub-domain only one secondary and one tertiary CBF is defined, assuming right hand sides of counterparts of (3) and (4) in the form of a sum of all interactions from the lower level CBFs. This opportunity has also been tested, but the results were not satisfactory.

The computed CBFs are then used as new basis and testing functions, which leads to a small matrix equation in comparison to initial matrix problem (1).

## 2.2 Wideband CBFs

One can see that, in order to obtain CBFs, we need to solve sets of linear equations (2) through (4). In a classical CBF method it is done at each frequency (or wavenumber $k$) of interest. Here, as in [6], we apply to this the AWE method, which is done with the following steps.

First, we expand both the impedance matrix $\boldsymbol{Z}$ and the excitation vector $\boldsymbol{V}$, into Taylor series around a chosen expansion point $k_0$:

$$\boldsymbol{Z}(k) \cong \sum_{q=0}^{Q} \boldsymbol{Z}_q (k - k_0)^q, \tag{5}$$

$$\boldsymbol{V}(k) \cong \sum_{q=0}^{Q} \boldsymbol{V}_q (k - k_0)^q \tag{6}$$

where $Q$ is a total number of Taylor coefficients. Also, above:

$$\boldsymbol{Z}_q = \frac{1}{q!} \frac{d^q \boldsymbol{Z}(k)}{dk^q}\bigg|_{k=k_0}, \tag{7}$$

$$\boldsymbol{V}_q = \frac{1}{q!} \frac{d^q \boldsymbol{V}(k)}{dk^q}\bigg|_{k=k_0}. \tag{8}$$

As indicated, obtaining expansions (5) and (6) requires calculating the proper derivatives of $\boldsymbol{Z}$ and $\boldsymbol{V}$ entries, with respect to $k$. For objects placed in free space, it can be done analytically, using the formulas given in ([9], p.706).

Next, we obtain Taylor series expansions for primary CBFs, applying AWE [7] – [9] to eq. (2):

$$\boldsymbol{Jp}_0^{(i)} = \left(\boldsymbol{Z}_{e,0}^{(i)}\right)^{-1} \boldsymbol{V}_0^{(i)}, \tag{9}$$

$$\boldsymbol{Jp}_q^{(i)} = \left(\boldsymbol{Z}_{e,0}^{(i)}\right)^{-1} \left[\boldsymbol{V}_q^{(i)} - \sum_{p=1}^{q} \boldsymbol{Z}_{e,p}^{(i)} \cdot \boldsymbol{Jp}_{q-p}^{(i)}\right], \quad q \geq 1 \tag{10}$$

where $\boldsymbol{Z}_{e,p}^{(i)}$ and $\boldsymbol{V}_q^{(i)}$, denote $p$-th or $q$-th Taylor coefficients of $\boldsymbol{Z}_e^{(i)}$ and $\boldsymbol{V}^{(i)}$, respectively. Those coefficients are extracted from $\boldsymbol{Z}_p$ and $\boldsymbol{V}_q$ in the same way as $\boldsymbol{Z}_e^{(i)}$ from $\boldsymbol{Z}$, and $\boldsymbol{V}^{(i)}$ from $\boldsymbol{V}$.

Then, total primary CBFs expansions are:

$$\boldsymbol{Jp}^{(i)}(k) \cong \sum_{q=0}^{Q} \boldsymbol{Jp}_q^{(i)} (k - k_0)^q. \tag{11}$$

Now, we form Taylor coefficients for right hand sides of (3):

$$\boldsymbol{R}_{n,q}^{(i)} = -\sum_{p=0}^{q} \boldsymbol{Z}_p^{(i,n)} \cdot \boldsymbol{Jp}_{q-p}^{(k)}, \quad q = 0, \ldots, Q \tag{12}$$

where again $\boldsymbol{Z}_p^{(i,n)}$ is $p$-th coefficient in the Taylor expansion of $\boldsymbol{Z}^{(i,n)}$.

Next, we obtain Taylor expansions for secondary CBFs, applying again AWE to (3), where excitation vector expansions are given by (12). Thus:

$$\boldsymbol{Js}_{n,0}^{(i)} = \left(\boldsymbol{Z}_{e,0}^{(i)}\right)^{-1} \boldsymbol{R}_{n,0}^{(i)}, \tag{13}$$

$$\boldsymbol{Js}_{n,q}^{(i)} = \left(\boldsymbol{Z}_{e,0}^{(i)}\right)^{-1} \left[\boldsymbol{R}_{n,q}^{(i)} - \sum_{p=1}^{q} \boldsymbol{Z}_{e,p}^{(i)} \cdot \boldsymbol{Js}_{n,q-p}^{(i)}\right], q \geq 1. \tag{14}$$

Again, we assumed the Taylor expansions for secondary CBFs in the form:

$$\boldsymbol{Js}_n^{(i)}(k) \cong \sum_{q=0}^{Q} \boldsymbol{Js}_{n,q}^{(i)} (k - k_0)^q. \tag{15}$$

Finally we repeat the procedure for equation (4), using counterparts of (12) – (14) with primary CBFs replaced by secondary ones, and secondary by tertiary functions.

At the final stage of getting the wideband approximations of CBFs, we represent them with Padé rational functions. The procedure for obtaining coefficients of those Padé expansions is given for example in ([9], pp.701-702) and will be not repeated here.

In order to apply the obtained CBF wideband expansions to find the (wideband) solution for the original problem, we first reconstruct CBFs for a given $k$ from their Padé expansions, then use those CBFs as basis and testing functions as in usual, single frequency CBF method. Note that to obtain final equation set we need to know also $\boldsymbol{Z}$ and $\boldsymbol{V}$ for the considered wavenumber $k$. We obtain them simply from (5) and (6), respectively. It is to be noted that during the whole procedure we only need to once invert the extended block matrices $\boldsymbol{Z}_{e,0}^{(i)}$ corresponding to matrices $\boldsymbol{Z}_e^{(i)}$, taken at $k = k_0$.

# 3. Computational Examples

## 3.1 Thin Wires

As an example of application of above procedure, we decided first to apply it to, useful for illustration purposes, case of thin wire radiator. This choice was dictated by the fact that it is relatively easy to show behavior of CBFs, if they correspond to one-dimensional structures. During computations, we used Pocklington equation and usual triangular basis and testing functions. We applied the exact kernel for situations, when the observation point belongs to source segment, and thin-wire kernel for the remaining cases.

We assumed that the radiating wire antenna, positioned along the z-axis, has a length $L$ = 1 m, and is center driven. The parameter $\Omega = 2\ln(L/a)$ was chosen to be 10.0 [10], which corresponds to $a = e^{-5L} = 6.738$ mm. The length of the antenna was divided into 121 equal segments, so we got $N = 120$ basis and testing functions. Odd number of segments enables excitation to be confined to the center segment, which causes two non-zero entries to appear in the excitation vector $\boldsymbol{V}$. As already mentioned, when using CBF method with $M > 2$ it results in the existence of zero $\boldsymbol{V}^{(i)}$ vectors for subdomains not covering the central segment. During computations with the CBF method, the initial subdomains were extended by $\lambda/8$ extensions ($\lambda$ being the wavelength corresponding to the AWE expansion point for wideband computations).

First, we checked single frequency CBF method with $M = 3$ and 5 subdomains. The results (input current magnitude versus wavenumber, for 1 V voltage generator) are given in Fig. 2. One can see that the CBF method results are indistinguishable from conventional method-of-moments solution. Next, we have arbitrarily chosen the expansion point $k_0 = 10.0$ (the mid-point of the frequency interval) and applied CBF-AWE method for five subdomains and various orders of Padé expansions. The example results are given in Fig. 3. Numbers in parenthesis next to "WCBF" (which stands for "wideband characteristic basis functions") denote degrees of numerator and denominator polynomials in Padé expansions. One can see that increasing the order of expansions does not enhance much the frequency interval in which the approximation is valid. To cover given frequency range it is therefore more reasonable to remain with lower order Padé expansions, but to add new expansion points.

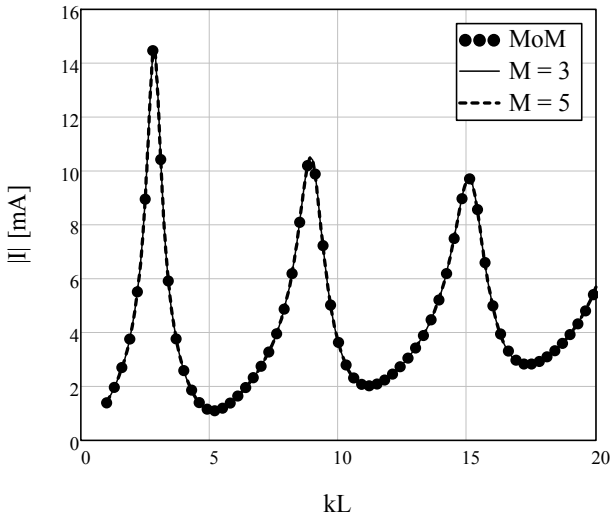


**Fig. 2.** Magnitude of antenna input current versus normalized wavenumber for two numbers of characteristic basis functions.

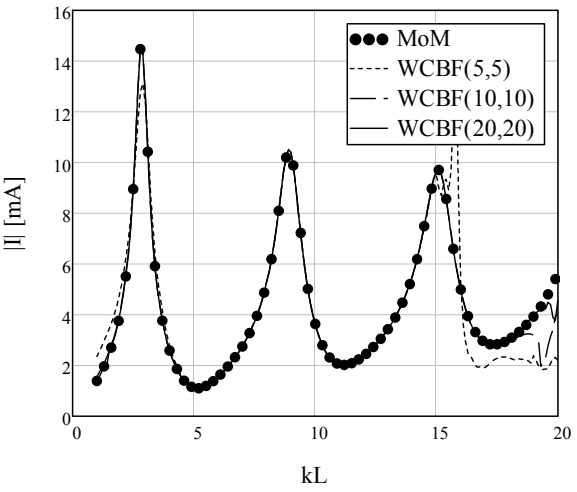


**Fig. 3.** Magnitude of antenna input current versus wavenumber for 5 segments and 21 wideband characteristic basis functions and various orders of Padé expansions.

Now, let's closer examine the behavior of CBF approximations at frequencies shifted away from the expansion point. From Fig. 3 it may be judged that the region of validity of the expansions with the lowest order (WCBF(5,5)) here is from $k$ = 3 to about 14 (assuming $L$ = 1.0 m). Let's confine our interest to values $k$ differing from $k_0$ by 3, i.e. $k$ = 7 and 13. For illustration, we use the case of $M$ = 3, for which we have 7 CBFs. In Fig. 4 and 5 current distributions corresponding to representative CBFs are shown. It can be seen that WCBFs, reconstructed from Padé approximations for given values of $k$, are the same as they direct (calculated separately for each frequency) counterparts.

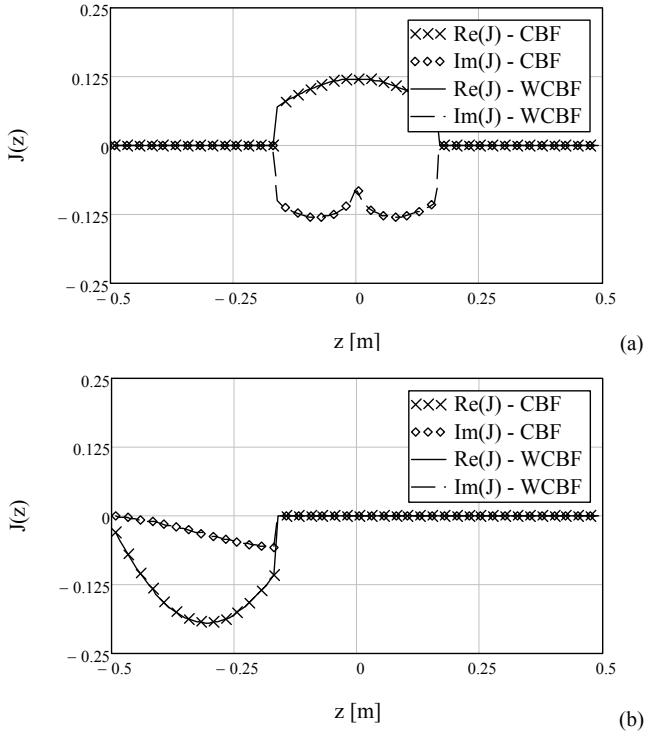


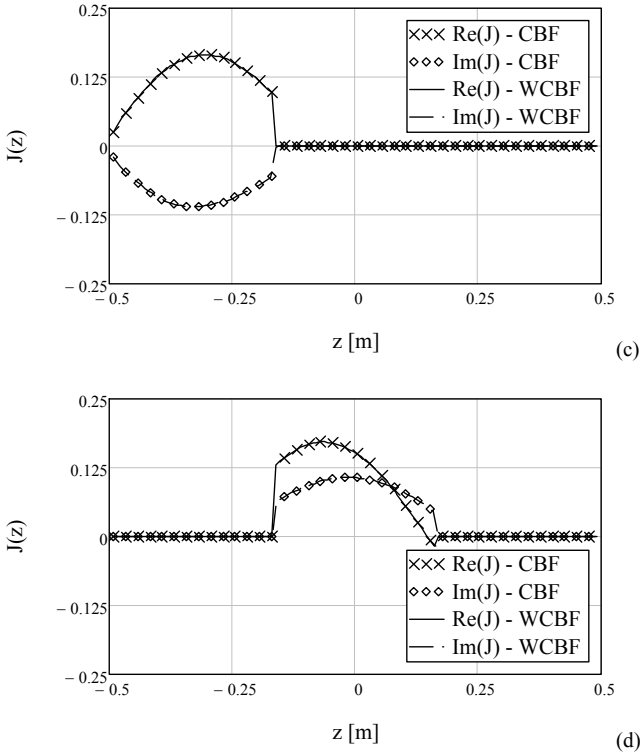


**Fig. 4.** Distribution of normalized characteristic basis functions along the wire with $L$ = 1 m, $\Omega = 10.0$: $\boldsymbol{Jp}^{(2)}$ (a), $\boldsymbol{Js}_2^{(1)}$ (b), $\boldsymbol{Jt}_{3,2}^{(1)}$ (c), $\boldsymbol{Jt}_{3,2}^{(2)}$ (d), at $k$ = 7.0.

Also the resulting total current distributions obtained with CBF or WCBF method are the same as those calculated with the classical MoM (Fig. 6).

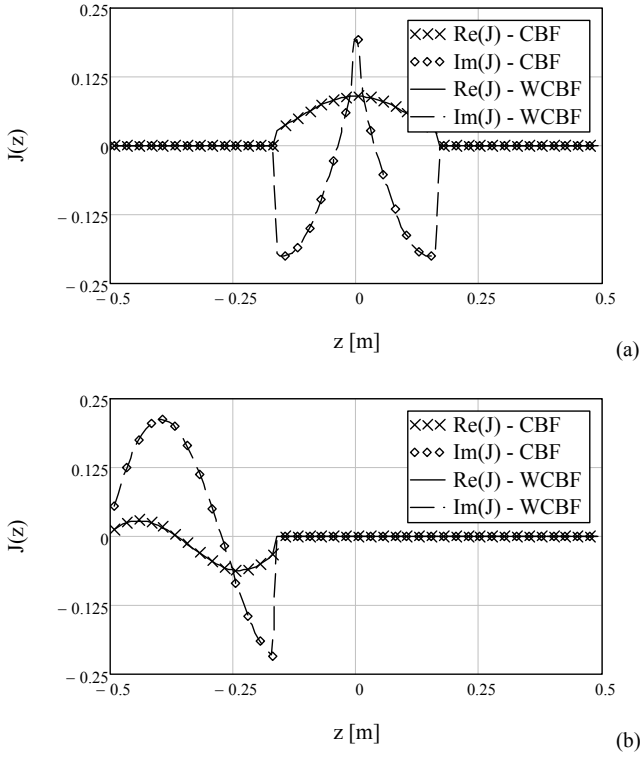

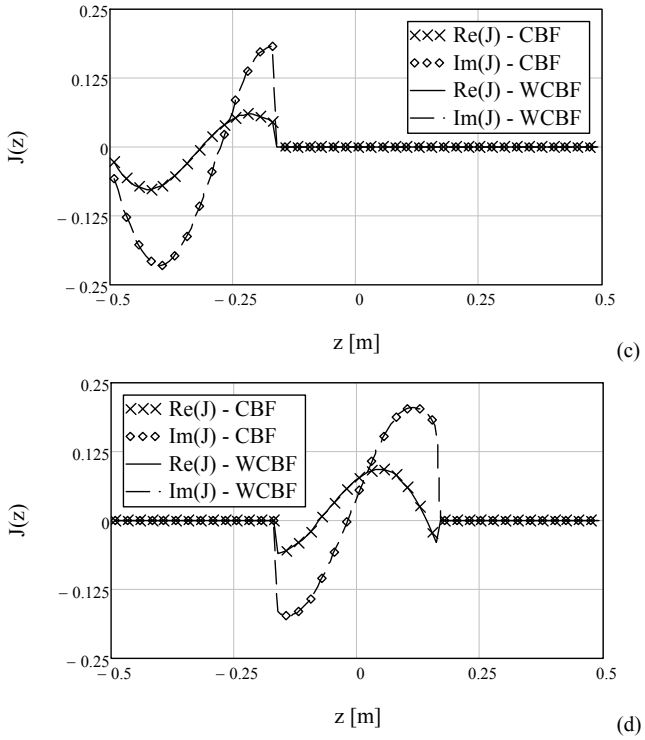


**Fig. 5.** Distribution of normalized characteristic basis functions along the wire with $L = 1$ m, $\Omega = 10.0$: $\boldsymbol{Jp}^{(2)}$ (a), $\boldsymbol{Js}_2^{(1)}$ (b), $\boldsymbol{Jt}_{3,2}^{(1)}$ (c), $\boldsymbol{Jt}_{3,2}^{(2)}$ (d), at $k = 13.0$.

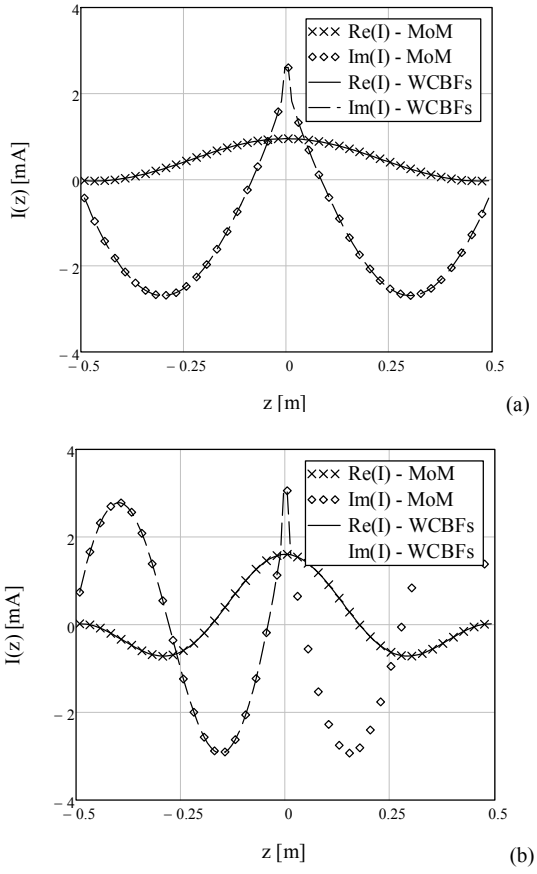


**Fig. 6.** Current distribution along the wire $L = 1$ m, $\Omega = 10.0$, for $k = 7.0$ (a), and $k = 13.0$ (b), obtained using classical MoM, and WCBFs constructed around $k_0 = 10$.

## 3.2 Surfaces

In the second example we applied CBF and WCBFs methods to analyze the slot antenna, with the slot made in the finite perfectly conducting plane (Fig. 7).

In order to construct characteristic basis functions, the structure has been divided into 9 blocks, as indicated in the figure. The structure, with dimensions $a = b = 2$ m, $L = 1$ m, $w = 0.02$ m, has been discretized into 4004 triangles, from which 5889 RWG [11] basis functions have been formed.

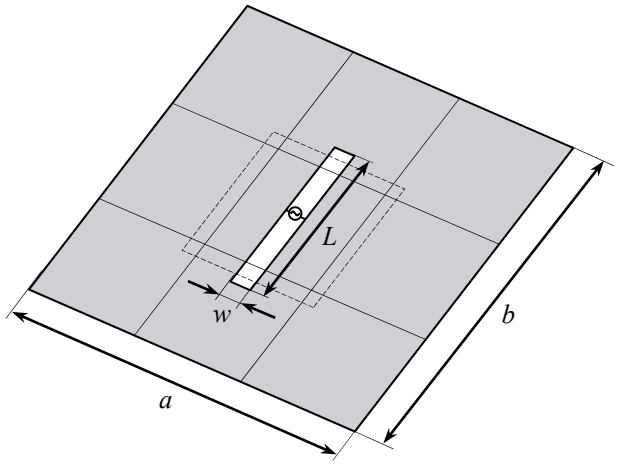


**Fig. 7.** Center driven rectangular slot antenna made in the finite perfectly conducting plane. The structure divided into 9 sub-domains, the dashed line indicates example extended block.

The overlapping margin was equal to 0.25 m, which lead to maximum number of basis function associated with "the biggest", central sub-domain equal to 2197 (the "smallest" in terms of that number were blocks associated with corners of the structure, with 1240 basis functions).

Fig. 8 shows computed input impedance of the slot antenna versus the (normalized) wavenumber. Lines corresponding to the classical method-of-moment solution and CBF solution are indistinguishable. WCBF solutions are built around the value $k_0L = 5.0$. Again, the increasing the order of Padé approximations from WCBF(5,5) to WCBF(15,15) does not lead to much wider validity region, therefore in the final computations, depicted in Fig. 9, we used WCBF(5,5), but with several expansion points and several smaller wavenumber intervals, indicated by different symbols.

In the case shown in Fig. 9, the computations were done in the following way: first, the expansion points near the ends of the considered band were chosen, namely $k_0L = 1.0$ and $k_0L = 9.0$. Then the results for the half of the interval were obtained from each expansion point. When the results from different expansions didn't agree at the mid-point ($k_0L = 5.0$ in the first iteration), this point was chosen as the new expansion point. The procedure was repeated until obtaining the coverage of the full interval.

The alternative procedure would require keeping the WCBFs and matrices (with derivatives) for every expan-

sion point in the memory, and only check the results at the mid-points. This would allow to not repeat computations for the frequency points which lie outside the validity interval of the given WCBF set.

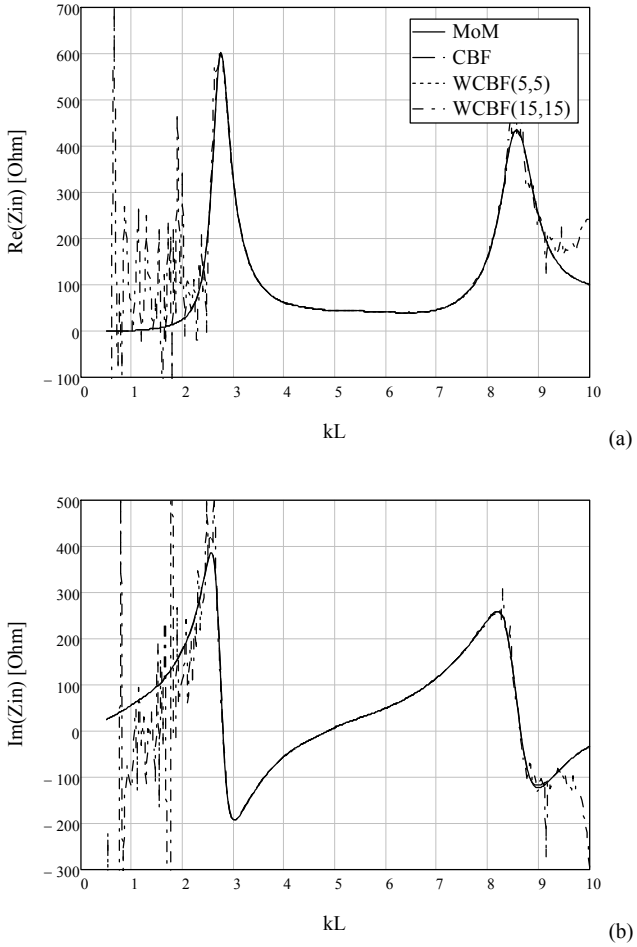


**Fig. 8.** Input impedance of the slot antenna from Fig. 7 with $a = b = 2$ m, $L = 1$ m, $w = 0.02$ m; (a) real part; (b) imaginary part; computations with standard MoM, CBF method, and WCBF method with the expansion point $k_0L = 5.0$.

Let's now consider the efficiency of the WCBF method. It is to be noted that, in contrast to the single frequency method, where the inversion of the $\boldsymbol{Z}_e^{(i)}$ sub-matrices required to obtain the CBFs via (2) through (4) has to be repeated at each frequency of interest, here we need to do this only at the expansion points $k_0$. For other frequencies, we only solve the final (small) set of equations with the number of unknowns equal to the number of CBFs. On the other hand, at each expansion point we need to compute not only the original moment matrix, but also its derivatives, which by the way must be stored in the memory. Also, at each frequency we need to restore the moment matrix and the excitation vector from their Taylor expansions – this is needed to form the final equation set. Therefore, the efficiency of the particular solution depends on the number of frequency points that could be covered using WCBF method, instead of standard MoM (or standard, single frequency CBF method).

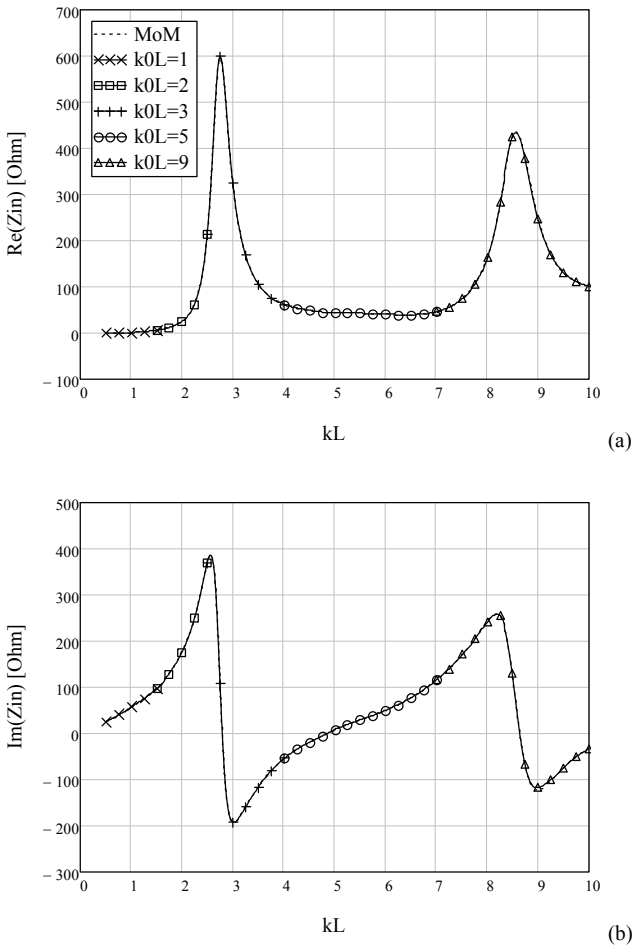


**Fig. 9.** Input impedance of the slot antenna from Fig. 7 with $a = b = 2$ m, $L = 1$ m, $w = 0.02$ m; (a) real part; (b) imaginary part; computations with standard MoM and WCBF method with the expansion points $k_0L = 1.0$; 2.0; 3.0; 5.0; and 9.0.

In the example, we made the comparisons using the workstation with Intel® Xeon® X5472 3.0 GHz CPU. For matrix inversion and solving linear equation sets Intel® MKL library was applied. In order to enable fair comparisons, single processor core was used. The computation times per single frequency were 104 s and 83.4 s in standard MoM and CBF methods, respectively.

In WCBF(5,5) method generation of WCBFs at single expansion point took about 1430 seconds, while the final solution at a single frequency required 8.5 seconds. We may conclude that:

- in the given example standard MoM and single frequency CBF methods have similar efficiency – this is due to the fact that the extended CBF sub-domains are relatively large in comparison with the total number of unknowns;
- in the example, the use of WCBF method makes sense when the number of frequency points per one expansion point is greater than 15;
- in the example, the total computation time (for 381 frequency points) using WCBF method (with 5 ex-

pansion points) was 3 times shorter than in the case of standard MoM; although this seems not a big speed-up ratio, it was still 3.6 hours of computations compared to 11 hours in the standard MoM and 8.8 in the case of single frequency CBF method.

When 2 processors/8 cores were used, the time of classical method computations was reduced to 57 seconds per frequency, which was due to parallelization present in Intel® MKL library routines. CBF method required 71 s per frequency. In the WCBF method the generation of WCBFs took about 1350 s per expansion point, and final computation required 8.1 s per frequency. Thus the total time in the WCBF method was 3.35 hours, which was 1.8 times shorter than in the classical method with 6 hours of computations.

# 4. Conclusion

In this paper we have checked the use of the wideband characteristic basis function method (AWE-CBF method) for radiation problems, involving localized excitation.

The validity of the idea has been verified on simple thin-wire antenna and slot antenna examples, but the method should be applicable to any method-of-moments solution, for which Taylor expansion of impedance matrix with respect to frequency is available.

# References

[1] PRAKASH, V. V. S., MITTRA, R. Characteristic basis function method: a new technique for efficient solution of method of moments matrix equations. *Microw. Opt. Tech. Lett.,* January 20, 2003, vol. 36, no. 2, p. 96–100.

[2] MITTRA, R., DU, K. Characteristic basis function method for iteration-free solution of large method of moments problems. *Progress in Electromagnetics Research B*, 2008, vol. 6, p. 307–336.

[3] PRAKASH, V. V. S. RCS computation over a frequency band using the characteristic basis and model order reduction method. *IEEE AP-S Symposium*, 22-27 June, 2003, vol. 4, p. 89–92.

[4] PRAKASH, V. V. S., YEO, J., MITTRA, R. An adaptive algorithm for fast frequency response computation of planar microwave structures. *IEEE Trans. Microwave Theory Techn.*, March 2004, vol. 52, no. 3, p. 920–926.

[5] ÖĞÜCÜ, G., MITTRA, R. An algorithm for fast frequency sweep of planar microwave circuits. In *Proc. IEEE Int. Symp. APS*, July 5–11, 2008.

[6] SUN, Y., DU, Y., SHAO, Y. Fast computation of wideband RCS using characteristic basis function method and asymptotic waveform evaluation technique. *Journal of Electronics (China)*, July 2010, vol. 27, no. 4, p. 463–467.

[7] PILLAGE, L. T., ROHRER, R. A. Asymptotic waveform evaluation for timing analysis. *IEEE Trans. Comput.-Aided Design*, Apr. 1990, vol. 9, no. 4, p. 352-366.

[8] REDDY, C. J., DESHPANDE, M. D., COCKRELL, C. R., BECK, F. B. Fast RCS computation over a frequency band using method of moments in conjunction with asymptotic waveform evaluation technique. *IEEE Trans. Antennas Propagat.*, Aug. 1998, vol. 46, no. 8, p.1229–1233.

[9] CHEW, W. C., MICHIELSSEN, E., SONG, J. M., JIN, J. M. *Fast and Efficient Algorithms in Computational Electromagnetics*. Boston, London: Artech House, 2001.

[10] TESCHE, F. M. The effect of the thin-wire approximation and the source gap model on the high-frequency integral equation solution of radiating antenna. *IEEE Trans. Antennas Propagat.*, March 1972, vol. 20, no. 2, p. 210–211.

[11] RAO, S. M., WILTON, D. R., GLISSON, A. W. Electromagnetic scattering by surfaces of arbitrary shape. *IEEE Trans. Antennas Propagat.*, May 1982, vol. AP-30, p. 409-418.

# About Authors

**Andrzej A. KUCHARSKI** was born in 1964. He received his M.Sc., Ph.D. and D.Sc. from Wroclaw University of Technology in 1988, 1994, and 2001, respectively. He is the Head of the Antenna Theory and Computational Electromagnetics Group in the Radiocommunications and Teleinformatics Department, Institute of Telecommunications, Teleinformatics and Acoustic, Wroclaw University of Technology, Poland. His research interests include computational electromagnetics in radiation and scattering problems.